INL/CON-11-22228
PREPRINT

Performance Assessment of Single Electrode-Supported Solid Oxide Cells Operating in the Steam Electrolysis Mode

IMECE 2011

X. Zhang
J. E. O'Brien
R. C. O'Brien
N. Petigny

November 2011

The INL is a
U.S. Department of Energy
National Laboratory
operated by
Battelle Energy Alliance

Proceedings of the ASME 2011 International Mechanical Engineering Congress & Exposition
IMECE2011
November 11-17, 2011, Denver, Colorado, USA

IMECE2011-64795

Performance Assessment of Single Electrode-Supported Solid Oxide Cells Operating in the Steam Electrolysis Mode

X. ZHANG
Idaho National Laboratory
Idaho Falls, ID, United States
Xiaoyu.Zhang@inl.gov

J.E. O'BRIEN
Idaho National Laboratory
Idaho Falls, ID, United States
James.OBrien@inl.gov

R.C. O'BRIEN
Idaho National Laboratory
Idaho Falls, ID, United States
Robert.OBrien@inl.gov

N. PETIGNY
Saint Gobain Advanced Materials
Cavaillon, France
Nathalie.Petigny@saint-gobain.com

ABSTRACT

An experimental study has been conducted to assess the performance of electrode-supported solid-oxide cells operating in the steam electrolysis mode for hydrogen production. Results presented in this paper were obtained from single cells, with an active area of 16 cm^2 per cell. The electrolysis cells are electrode-supported, with yttria-stabilized zirconia (YSZ) electrolytes (~10 μm thick), nickel-YSZ steam/hydrogen electrodes (~1400 μm thick), and modified LSM or LSCF air-side electrodes (~90 μm thick). The purpose of the present study is to document and compare the performance and degradation rates of these cells in the fuel cell mode and in the electrolysis mode under various operating conditions. Initial performance was documented through a series of voltage-current (VI) sweeps and AC impedance spectroscopy measurements. Degradation was determined through long-term testing, first in the fuel cell mode, then in the electrolysis mode. Results generally indicate accelerated degradation rates in the electrolysis mode compared to the fuel cell mode, possibly due to electrode delamination. The paper also includes details of an improved single-cell test apparatus developed specifically for these experiments.

INTRODUCTION

Large-scale non-fossil hydrogen production based on high-temperature electrolysis is under investigation as an alternative to steam methane reforming, which accounts for about 95% of current hydrogen in the United States [1]. Most hydrogen consumption in North America is for petroleum refining, ammonia-based fertilizer production, and chemical industries [2]. Demand for hydrogen is increasing, primarily due to refining requirements for increasingly low quality petroleum resources such as oil sands and heavy crudes. In terms of natural gas supply, the proved reserves of natural gas in U.S. at 2009 is 272.5 trillion cubic feet [3], which corresponds to only 13 years of supply based on 2009 U.S. production level (20.955 trillion cubic feet) [3]. Domestic hydrogen demand in 2040 is projected to increase to 64 million metric tons [4], compared to 9 million metric tons in 2003 [2]. As the demand for hydrogen keeps increasing, the U.S. cannot rely solely on natural gas for hydrogen production. The greatest energy security vulnerability for the US is in the area of transportation fuels. Domestic hydrogen production based on nuclear or renewable energy allows these carbon-free energy resources to contribute to the transportation sector through refining of petroleum, synthetic fuels production, or ultimately as a direct vehicle fuel.

From a long-term perspective, sustainable methods must be developed for large-scale hydrogen production [5]. Non-fossil methods of hydrogen production are reviewed in [6]. Among all the sustainable hydrogen production methods, high temperature electrolysis (HTE) is one of the promising technologies that can be used for large-scale hydrogen production [7].

The US Department of Energy, Office of Nuclear Energy has supported development of HTE at the Idaho National Laboratory (INL) since 2003. INL has demonstrated HTE at the 15 kW scale with a hydrogen production rate in excess of 5000 NL/hr [8]. HTE research at INL is currently supported by the DOE Office of Nuclear Energy under the Next Generation Nuclear Plant (NGNP) Program [9]. However, technical barriers need to be resolved before

commercialization of HTE technology. The major issue for HTE is long-term performance degradation of the solid oxide electrolysis cells (SOECs). Although common solid oxide fuel cells (SOFCs) can be reversely operated in electrolysis mode, they usually exhibit much higher degradation rates in the electrolysis mode than in fuel cell mode [10-12]. More fundamental research on single cells needs to be done to characterize the degradation mechanisms and mitigate the degradation of SOECs.

In this paper, two batches of single cells with different air electrodes have been investigated experimentally. Initial performance and long term durability tests were conducted in both the fuel cell and electrolysis modes of operation. The purpose of the experiments was to compare the long term performance of the cells in two operating modes.

EXPERIMENTAL APPARATUS

The solid oxide cells used for this study are electrode-supported, with yttria-stabilized zirconia (YSZ) electrolytes (~10 μm thick), nickel-YSZ steam/hydrogen electrodes (~1400 μm thick), and modified lanthanum strontium manganite (LSM) or lanthanum strontium cobalt ferrite (LSCF) air-side electrodes (~90 μm thick). All of the cells were provided by Saint Gobain Advanced Materials (Cavaillon, France). The cells are square, 5 × 5 cm in dimension with 16 cm^2 active area.

Compared to the previous single-cell test apparatus, described in [13], the cell fixture and test stand have been redesigned to simplify the assembly procedure, improve the interface contact, and allow for operation at higher current densities. The new testing apparatus can be used to test both 5 × 5 cm single cells and small stacks.

The latest design of the cell fixture is shown in an exploded view in Fig. 1. A hydrogen/steam mixture is fed from the bottom through a 1/4 in coiled Inconel tube into the inlet hole in the bottom of the Hastelloy-X (HastX) base plate. The flow then passes through a slot at the bottom of the Alumina cell holder. The nickel plate works as the current collector for the steam-hydrogen electrode. A corrugated nickel flow field provides multiple flow channels for the steam-hydrogen flow and electrical conduction. A nickel felt is placed between the electrode and the nickel flow field to minimize the electrode/flow field contact resistance. The Ni felt and flow field are trimmed to fit the size of the Ni plate sitting in the recess of the cell holder. After passing along the bottom of the cell, the flow exits through another slot and vents out via a 3/8-in inconel tube. The outlet tube is sized larger than the inlet tube to minimize the back pressure on the cell seal. A mica/glass cell gasket is placed on the "window frame" between the cell holder and the cell for sealing.

On the air side of the cell, a gold-plated perforated inconel plate is used as the current collector and air flow distributer. Air is introduced through a tube that is welded to the inconel plate. Air flow is distributed along the air side of the cell through an array of flow channels milled into the bottom of the inconel plate. Air exhaust gas vents out to the furnace. A gold mesh is placed between the air electrode and the plate to minimize ohmic loss and to further improve air flow distribution. The top conductor / air flow distributor consists of three parts. The tube is welded and protruded slightly into the center hole of the upper inconel plate. Another inconel plate was machined with the flow channels and through-plate holes. These two plates were then welded together. Gold plating was applied to the inconel surfaces that are exposed to the furnace hot zone to minimize oxidation.

In the previous design, a silver-palladium lower plate was fabricated and laser welded to the upper inconel plate and tube. The thought was to eliminate chromium poisoning on the air electrode. However, oxidation of the inconel plate became an issue in long term tests and gold plating was used in the present design.

A fixed compression load is applied to the solid oxide cell by means of weights, as shown in the test stand overview, Fig. 2. The load is transferred via an alumina tube from the dead weights to the top cell contact plate. This load simultaneously compresses the cell against the nickel felt, flow field and current collector on the bottom steam/hydrogen side of the cell and against the gold mesh on the air side. It also compresses the cell against the seal around the outer edge of the cell which rests on the shelf milled into the alumina cell holder. The HastX weight plates are held in alignment outside of the furnace by the upper portion of the threaded rods which

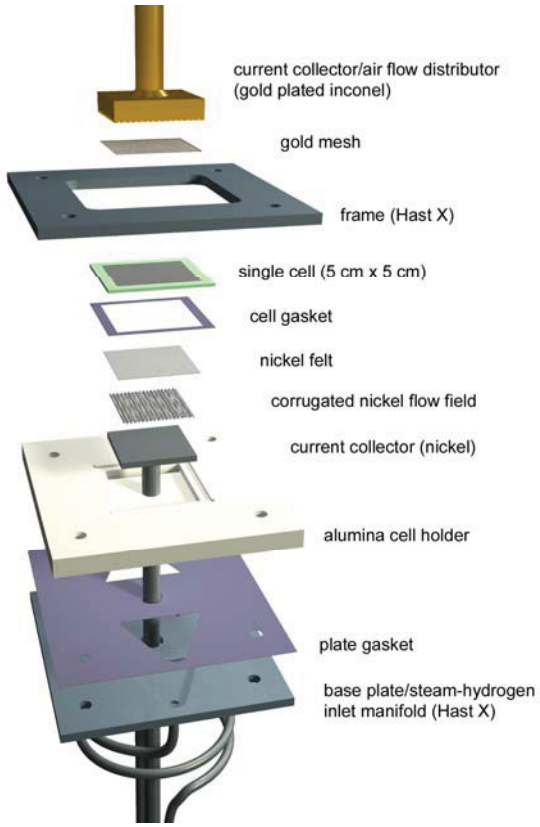

Figure 1. Exploded view of the cell fixture.

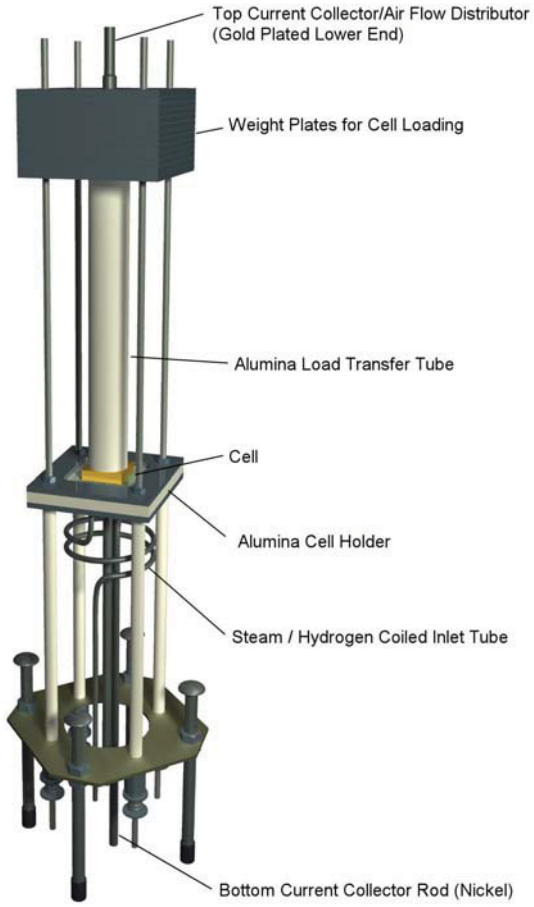

Figure 2. Test stand overview.

extend upward for this purpose.

The compressive load can also be applied by means of springs. Spring loading is more compact and easier to implement than adding weights. However, a major drawback of using springs is that the spring compression needs to be adjusted during heatup due to thermal expansion of the supporting rods. That becomes the advantage of dead weights since it maintains a constant load during heatup, independent of thermal expansion.

A photograph of the test stand installed in the furnace base is shown in Fig. 3. Note that the upper part of the alumina load transfer tube is located outside of the furnace. So the weights stay outside of the hot zone. Holes were drilled in the bottom of the kiln for pass-through of the flow tubes, the alumina spacer rods, the nickel current collector rod and instrumentation.

AC impedance spectroscopy was used to characterize the electrochemical behavior of the SOECs. Impedance measurements were obtained using a Solartron Modulab 2100A system. Impedance data were acquired in fuel cell mode, electrolysis mode, and open circuit condition. During the long term tests, impedance measurements were conducted periodically to characterize the degradation of the cells.

A process flow diagram for the experimental apparatus

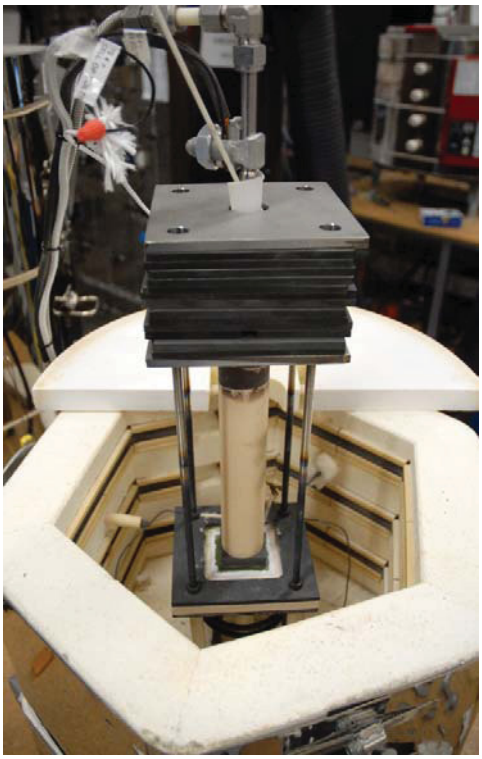

Figure 3. Single cell test stand installed in furnace.

used for single-cell testing is presented in Fig. 4. Primary components include gas supply cylinders, mass-flow controllers, a heated water-bath humidifier, on-line dewpoint sensors, temperature and pressure measurement, high temperature furnace, and the solid oxide electrolysis cell. Nitrogen is used as an inert carrier gas. Inlet flow rates of nitrogen, hydrogen, and air are established by means of precision mass-flow controllers. Hydrogen is included in the inlet flow as a reducing gas in order to prevent oxidation of the Nickel cermet electrode material. Air flow to the cell is supplied by the shop air system, after passing through a two-stage extractor / dryer unit. The hydrogen-side inlet gas mixture, consisting of hydrogen and nitrogen is mixed with steam by means of a heated humidifier. Dewpoint temperatures of the nitrogen / hydrogen / steam gas mixture exiting the humidifier are monitored continuously using two precision dewpoint sensors, one upstream and one downstream of the cell. The dewpoint sensors provide an independent measure of steam production (fuel cell mode) or consumption (electrolysis mode). All gas lines located downstream of the humidifier are heat-traced in order to prevent steam condensation.

TEST PROCEDURE

Each single cell undergoes three steps during the test, including initial heatup and cell reduction, performance characterization, and long-term testing. In the first step, the single cell temperature is ramped up to 850 or 900°C. Nickel

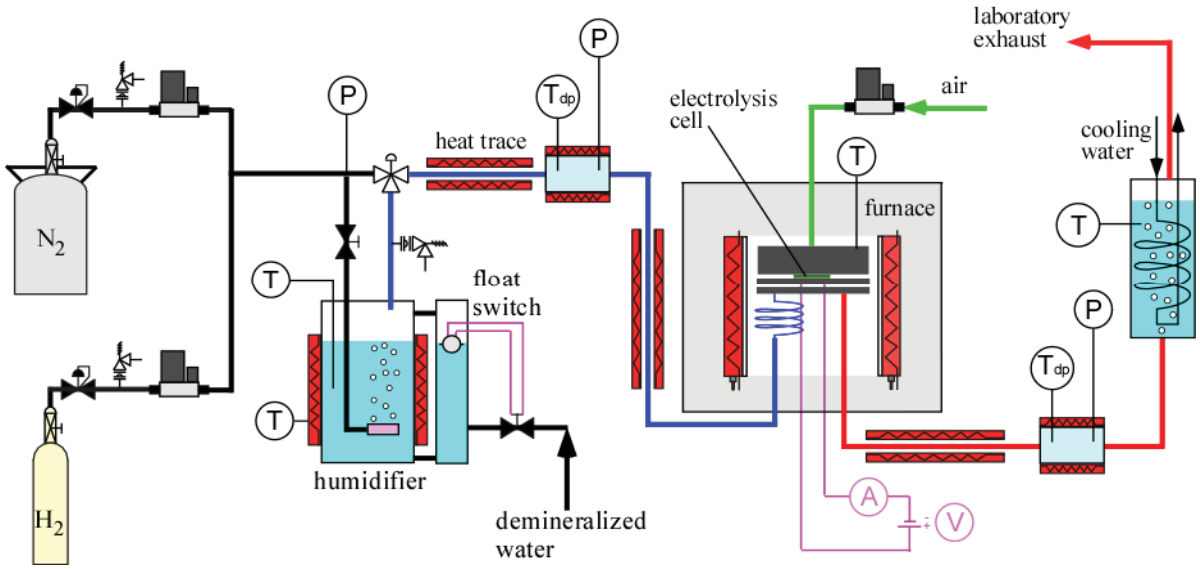

Figure 4. Process flow diagram for single-cell test apparatus.

oxide in the steam/hydrogen electrode is reduced to nickel metal by slowly introducing successively greater amounts of dry hydrogen flow. After reduction, the cells were operated at 850°C for testing.

Initial cell performance is evaluated by means of a series of voltage-current (V-I) sweeps with different steam content at the steam/hydrogen inlet. Operating conditions during V-I sweeps are listed in Table I.

After the performance evaluation, the cells were operated in fuel cell mode for over 100 hours. Then a few intermediate performance measurements were performed, followed by long-term testing in the electrolysis mode. The operating conditions during long term tests are listed in Table II.

AC impedance measurements were performed following the initial DC sweeps as well as periodically during the long-term tests. The excitation frequency range was 100 kHz – 0.1 Hz.

RESULTS AND DISCUSION

Fig. 5a shows the results of V-I sweeps for the single cells with modified LSM (black curves) and LSCF (red curves) air electrodes at different inlet dew point values. The curves show the effect of the steam content on initial cell performance. Curves representing higher steam content show more linear trends both in fuel cell and electrolysis modes. The nonlinearity in the curves at low steam content is associated with the high sensitivity of the Nernst potential to small changes in average steam content. Also, in the electrolysis mode, higher current densities can lead to steam starvation if the average steam content is low. A high inlet dew point temperature, typically 60°C or higher is suggested for long-term operation in the electrolysis mode [12]. Based on the slopes of the V-I curves, the single cell with the LSCF air electrode demonstrated better performance than the one with modified LSM electrode.

Calculated values of "apparent" area-specific resistances (ASRs) based on the V-I sweeps in Fig. 5a are shown in Fig. 5b. Apparent *ASR* is defined as follows:

$$ASR = \frac{V_{op} - V_{oc}}{i} \quad (1)$$

Where V_{op} is the cell operating voltage, V_{oc} is the open-cell voltage, and i is the current density.

The figure shows that the *ASR* curves remain flat at high steam content in both modes, while becoming significantly curved especially in electrolysis mode as steam content decreases. At high steam content, the ASR values are similar in the fuel cell and electrolysis modes. At 70°C T_{dpi} (35.4% steam content), ASR values for the cell with modified LSM air electrode and the one with LSCF air electrode are around 0.35 Ω.cm^2 and 0.2 Ω.cm^2, respectively.

Following the initial performance evaluation, the single cells are put in long-term operation in fuel cell mode. Fig. 6 shows the result of a long-term test of the single cell with modified LSM air electrode. The cell is operated galvanostatically at 0.5 A/cm^2 at 850 °C. The cell performance

Table I. Operating conditions during V-I sweeps

Cell °C	H_2 sccm	N_2 sccm	Air sccm	Dew Point °C
800, 850	500	500	1000	20, 50, 70

Table II. Operating conditions during long term tests

Cell °C	H_2 sccm	N_2 sccm	Air sccm	Dew Point °C	Current A/cm^2
800, 850	500	500	1000	70	0.5

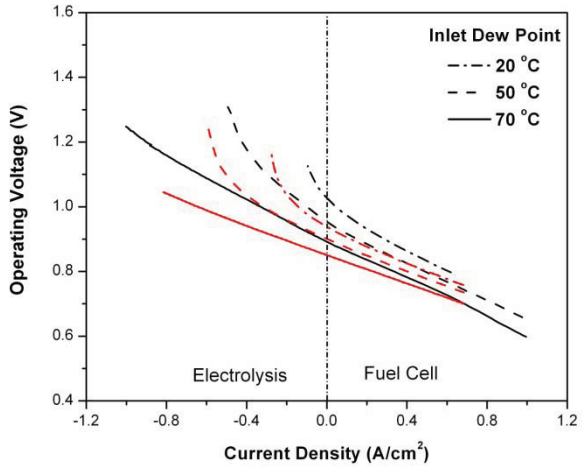

(a)

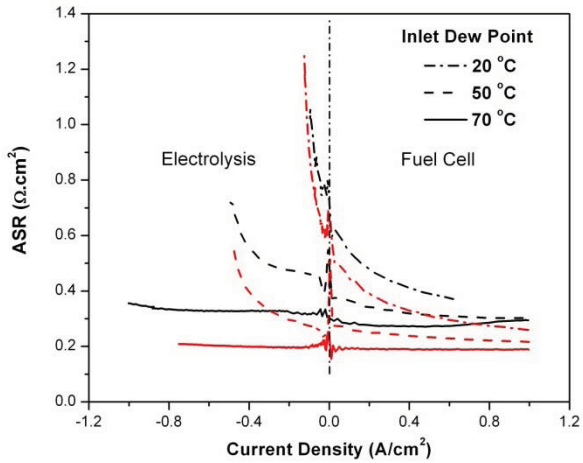

(b)

Figure 5. Polarization curves and calculated ASR values in fuel cell and electrolysis modes, showing the effect of steam content. Black and red curves show the results of modified LSM and LSCF air electrode, respectively.

is very stable in fuel cell mode with almost zero degradation. However, after switching to electrolysis mode, the cell exhibits rapid performance degradation. The test was terminated after only 5 hours operation in electrolysis mode.

More detailed information related to cell performance can be obtained from the impedance spectra. Impedance measurements were performed before and after the long-term fuel cell test, and after 5 hours operation in electrolysis mode. Fig. 7 shows Nyquist plots of the impedance spectra. The intercept of the spectra at high frequency with the real axis represents the ohmic resistance including electrolyte resistance. The results indicate that the electrolyte remains stable in electrolysis mode. The semi-circles at low frequencies characterize the electrochemical behavior of the electrodes. The SOEC spectrum shows that after operating in electrolysis mode for only 5 hours, the shape of semi-circle at low

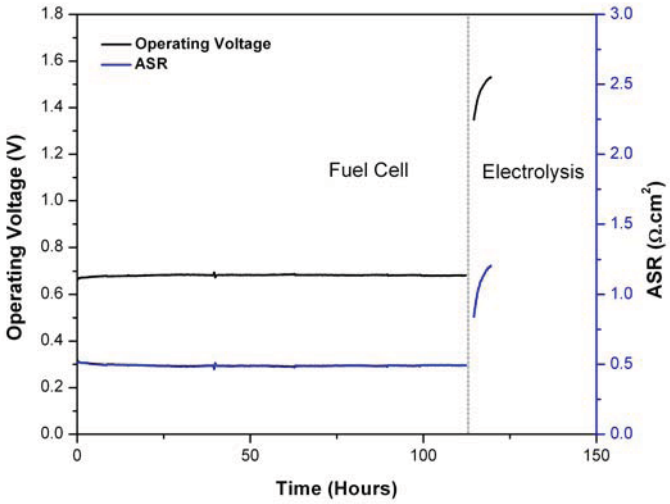

Figure 6. Long term test of the single cell with modified LSM air electrode. The cell is operated at 0. 5 A/cm^2 at 850 °C.

frequencies is greatly altered, consistent with significant degradation of electrode performance after switching to electrolysis mode.

Fig. 8 shows the results of the long-term test of the single cell with LSCF air electrode. The cell was operated gavalostatically at 0.5 A/cm^2 at 850 °C. The cell was operated in fuel cell mode for 180 hours before switching to electrolysis mode. Significant degradation was again observed in the electrolysis mode and the test was shut down after running in electrolysis mode for less than 10 hours.

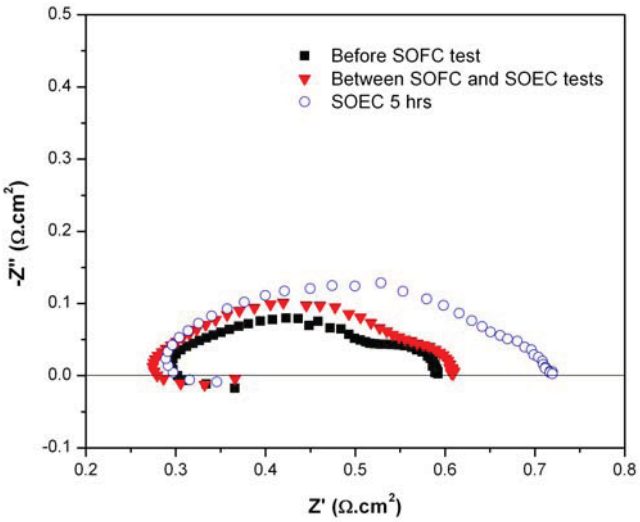

Figure 7. Nyquist plots of the impedance spectra measured during long term tests in fuel cell and electrolysis modes at open circuit conditions. The measurements are performed during the test shown in Fig. 6.

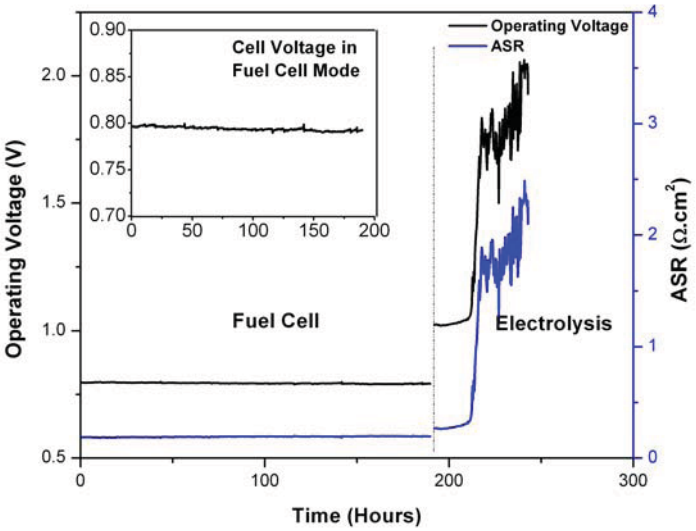

Figure 8. Long term test of the single cell with LSCF air electrode. The cell is operated at 0.5 A/cm^2 at 850 °C.

SUMMARY

A newly designed apparatus has been developed for testing of single solid oxide cells in both fuel cell and electrolysis modes of operation. Performance and durability evaluation of electrode-supported electrolysis cells with modified LSM and LSCF air electrodes has been completed. The cells demonstrate excellent initial performance in both modes with high steam content. Long term durability tests were conducted but significant apparent degradation was observed in electrolysis mode, primarily due to problems with electrode degradation.

ACKNOWLEDGMENTS

This work was supported by the U.S. Department of Energy, Office of Nuclear Energy, Nuclear Hydrogen Initiative and Next Generation Nuclear Plant Programs under DOE Operations Office Contract DE-AC07-05ID14517.

REFERENCES

1. National Academies, National Research Council and National Academy of Engineering, The hydrogen economy: opportunities, costs, barriers, and R&D needs, National Academies Press, Washington, 2004.
2. Basic Research Needs for the Hydrogen Economy, Report of the basic energy sciences workshop on hydrogen production, storage, and use, May13-15, 2003, available at http://www.sc.doe.gov/bes/reports/files/NHE_rpt.pdf
3. International Energy Statistics, U.S. Energy Information Admn, available at http://www.eia.gov/countries/data.cfm
4. Hydrogen, Fuel Cells & Infrastructure Technologies Program, 2.0 Program Benefits, 2007, U.S. Department of Energy, available at http://www1.eere.energy.gov/hydrogenandfuelcells/mypp/
5. Turner, J.A., "Sustainable Hydrogen Production," Science, **305**, pp. 972-974, 2004
6. Holladay, J.D., Hu, J., King, D.L., and Wang, Y., "An overview of hydrogen production technologies," Catalysis Today, **305**(4), pp. 244-260, 2009.
7. O'Brien, J. E., "Review of the Potential of Nuclear Hydrogen for Addressing Energy Security and Climate Change," Second Int. Mtg. of the Safety and Technology of Nuclear Hydrogen Production, Jun. 13-17, 2010, San Diego, CA.
8. Stoots, C. M., O'Brien, J. E., Condie, K., Moore-McAteer, L., Housley, G. K., Hartvigsen, J. J., and Herring, J. S., "The High-Temperature Electrolysis Integrated Laboratory Experiment," Nuclear Technology, April, 2009.
9. Southworth, F., Macdonald, P. E., Harrell, D. J., Park, C. V., Shaber, E. L., Holbrook, M. R., and Petti, D. A., "The Next Generation Nuclear Plant (NGNP) Project," Proceedings, Global 2003, pp. 276-287, 2003.
10. Hauch, A., Jensen, S. H., Ramousse, S., and Mogensen, M., "Performance and Durability of Solid Oxide Electrolysis Cells," Journal of the Electrochemical Society, **153**(9), pp. A1741-A1747, 2006
11. O'Brien, J. E., Stoots, C. M., Herring, J. S., and Hartvigsen, J. J., "Performance of Planar High-Temperature Electrolysis Stacks for Hydrogen Production from Nuclear Energy," Nuclear Technology, **158**, pp. 118 - 131 ,2007
12. Mawdsley, J. R., David Carter, J., Jeremy Kropf, A., Yildiz, B., and Maroni, V. A., "Post-test evaluation of oxygen electrodes from solid oxide electrolysis stacks ," International Journal of Hydrogen Energy, **34**(9), pp. 4198-4207, 2009
13. O'Brien, J. E., and Stoots, C. M., "High Temperature Electrolysis using Electrode-Supported Cells," European Fuel Cell Forum 2010, June 29 - July 2, 2010, Lucerne, Switzerland